hp-Version Trefftz Discontinuous Galerkin Method for the Homogeneous Helmholtz Equation

Scott Congreve

Fakultät für Mathematik, Universität Wien

Joint work with
Ilaria Perugia (Universität Wien)
Paul Houston (University of Nottingham)

Austrian Numerical Analysis Day 2016

Overview

universität wien

Let $\Omega \subset \mathbb{R}^d$, $d = 2, 3$ be a bounded polygonal/polyhedral domain.

$$
\begin{aligned}
-\Delta u - k^2 u &= 0 && \text{in } \Omega, \\
u &= 0 && \text{on } \Gamma_D, && \text{(sound-soft scattering)} \\
\nabla u \cdot \boldsymbol{n} &= 0 && \text{on } \Gamma_N, && \text{(sound-hard scattering)} \\
\nabla u \cdot \boldsymbol{n} + ik\vartheta u &= g_R && \text{on } \Gamma_R.
\end{aligned}
$$

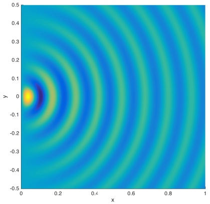

Acoustic Wave Prop.

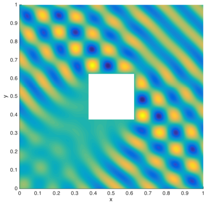

Sound-soft Scattering

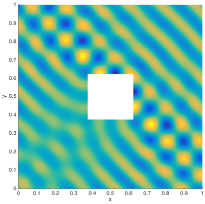

Sound-hard Scattering

FEM for Helmholtz

Problems with FEM:

- Number of *degrees of freedom* required to obtain given accuracy increases with wave number k.
- h-version FEM affected by pollution effect [Babuška & Sauter, 2000]:

$$\|u - u_h\| \leq C(k) \inf_{v_h \in V(\mathcal{T}_h)} \|u - v_h\|$$

$C(k)$ is an increasing function in k.

Problems with FEM:

- Number of *degrees of freedom* required to obtain given accuracy increases with wave number k.
- h-version FEM affected by pollution effect [Babuška & Sauter, 2000]:

$$\|u - u_h\| \leq C(k) \inf_{v_h \in V(\mathcal{T}_h)} \|u - v_h\|$$

$C(k)$ is an increasing function in k.

We incorporate information about the frequency into the finite element space to attempt to reduce computation cost.

Polynomial DG Finite Element Spaces: DGFEM uses polynomial basis functions defined on a reference element $\widehat{K}$:

$$V_q^{DG}(\mathcal{T}_h) := \{v \in L^2(\Omega) : v|_K \circ F_K \in \mathcal{S}_{q_K}(\widehat{K}), K \in \mathcal{T}_h\}.$$

Trefftz FEM Spaces

Polynomial DG Finite Element Spaces: DGFEM uses polynomial basis functions defined on a reference element $\widehat{K}$:

$$V_q^{DG}(\mathcal{T}_h) := \{v \in L^2(\Omega) : v|_K \circ F_K \in \mathcal{S}_{q_K}(\widehat{K}), K \in \mathcal{T}_h\}.$$

Trefftz Finite Element Space: Use basis functions defined element-wise based on general solutions to the PDE.
First define the local Trefftz spaces

$$T(K) := \{v|_K : -\Delta u - k^2 u = 0\}$$

and let

$$T(\mathcal{T}_h) := \{v \in L^2(\Omega) : v|_K \in T(K), K \in \mathcal{T}_h\}.$$

Polynomial DG Finite Element Spaces: DGFEM uses polynomial basis functions defined on a reference element $\widehat{K}$:

$$V_q^{DG}(\mathcal{T}_h) := \{v \in L^2(\Omega) : v|_K \circ F_K \in \mathcal{S}_{q_K}(\widehat{K}), K \in \mathcal{T}_h\}.$$

Trefftz Finite Element Space: Use basis functions defined element-wise based on general solutions to the PDE.
First define the local Trefftz spaces

$$T(K) := \{v|_K : -\Delta u - k^2 u = 0\}$$

and let

$$T(\mathcal{T}_h) := \{v \in L^2(\Omega) : v|_K \in T(K), K \in \mathcal{T}_h\}.$$

We let $V_p(K) \subset T(K)$ be a finite dimensional local space; then, the Trefftz FE Space is given by

$$V_p(\mathcal{T}_h) := \{v \in T(\mathcal{T}_h) : v_K \in V_p(K), K \in \mathcal{T}_h\}.$$

Plane Waves

$$V_p(K) = \left\{ v : v(\boldsymbol{x}) = \sum_{\ell=1}^{p_K} \alpha_\ell \mathrm{e}^{ik\boldsymbol{d}_\ell \cdot (\boldsymbol{x} - \boldsymbol{x}_K)}, \alpha_\ell \in \mathbb{C} \right\}$$

where p_K is the number of *degrees of freedom* for the element K, $\boldsymbol{d}_l$, $l = 1, \cdots, N_K$ are p_K (roughly) evenly spaced unit direction vectors, and $\boldsymbol{x}_K$ is the centre of the element.

Plane Waves

$$V_p(K) = \left\{ v : v(\boldsymbol{x}) = \sum_{\ell=1}^{p_K} \alpha_\ell \mathrm{e}^{ik\boldsymbol{d}_\ell \cdot (\boldsymbol{x} - \boldsymbol{x}_K)}, \alpha_\ell \in \mathbb{C} \right\}$$

where p_K is the number of *degrees of freedom* for the element K, $\boldsymbol{d}_l$, $l = 1, \cdots, N_K$ are p_K (roughly) evenly spaced unit direction vectors, and $\boldsymbol{x}_K$ is the centre of the element.

Trefftz DG has less degrees of freedom than high-order polynomials for the same accuracy.

Basis Functions	2D	3D
DG ($\mathcal{P}_q$)	$(q+1)(q+2)/2$	$(q+1)(q+2)(q+3)/6$
DG ($\mathcal{Q}_q$)	$(q+1)^2$	$(q+1)^3$
Trefftz DG	$2q+1$	$(q+1)^2$

Number of Degrees of Freedom

Plane Waves

$$V_p(K) = \left\{ v : v(\boldsymbol{x}) = \sum_{\ell=1}^{p_K} \alpha_\ell \mathrm{e}^{ik\boldsymbol{d}_\ell \cdot (\boldsymbol{x} - \boldsymbol{x}_K)}, \alpha_\ell \in \mathbb{C} \right\}$$

where p_K is the number of *degrees of freedom* for the element K, $\boldsymbol{d}_l$, $l = 1, \cdots, N_K$ are p_K (roughly) evenly spaced unit direction vectors, and $\boldsymbol{x}_K$ is the centre of the element.

Trefftz DG has less degrees of freedom than high-order polynomials for the same accuracy.

Basis Functions	2D	3D
DG ($\mathcal{P}_q$)	$(q+1)(q+2)/2$	$(q+1)(q+2)(q+3)/6$
DG ($\mathcal{Q}_q$)	$(q+1)^2$	$(q+1)^3$
Trefftz DG	$2q+1$	$(q+1)^2$

Number of Degrees of Freedom

Direction Vectors ($q = 3$):

2D

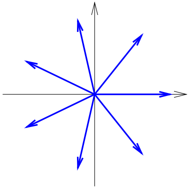

3D

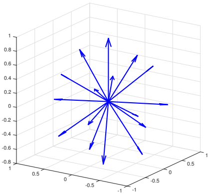

[Sloan & Womersley, 2004]

TDG/DG FEM Comparison

Consider the smooth (analytic) solution (for Acoustic Wave Propagation)

$$u(r,\theta) = \mathcal{J}_1(kr)\cos(\theta)$$

for $k = 20$ on the domain $\Omega = (0,1) \times (-1/2, 1/2)$.

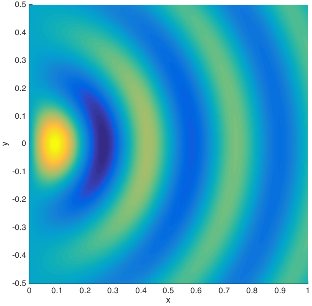

Analytical Solution
(Real Part)

Consider the smooth (analytic) solution (for Acoustic Wave Propagation)

$$u(r,\theta) = \mathcal{J}_1(kr)\cos(\theta)$$

for $k = 20$ on the domain $\Omega = (0,1) \times (-1/2, 1/2)$.
We solve using both a DGFEM (solid line) and Trefftz DGFEM (dashed).

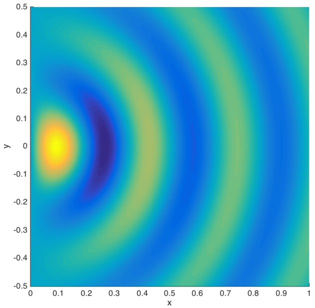

Analytical Solution
(Real Part)

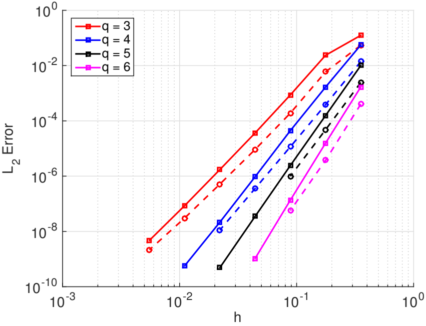

$\|u - u_{hp}\|_{L^2(\Omega)}$ vs. h
(h-refinement)

Consider the smooth (analytic) solution (for Acoustic Wave Propagation)

$$u(r,\theta) = \mathcal{J}_1(kr)\cos(\theta)$$

for $k = 20$ on the domain $\Omega = (0,1) \times (-1/2, 1/2)$.
We solve using both a DGFEM (solid line) and Trefftz DGFEM (dashed).

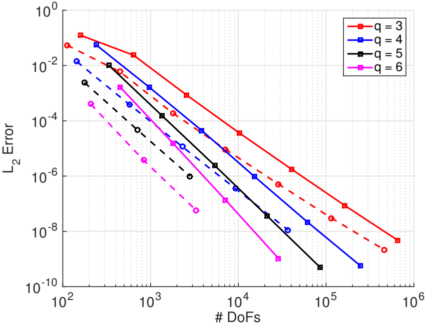

$\|u - u_{hp}\|_{L^2(\Omega)}$ vs. Degrees of Freedom (h-refinement)

TDG/DG FEM Comparison

Consider the smooth (analytic) solution (for Acoustic Wave Propagation)

$$u(r,\theta) = \mathcal{J}_1(kr)\cos(\theta)$$

for $k = 20$ on the domain $\Omega = (0,1) \times (-1/2, 1/2)$.
We solve using both a DGFEM (solid line) and Trefftz DGFEM (dashed).

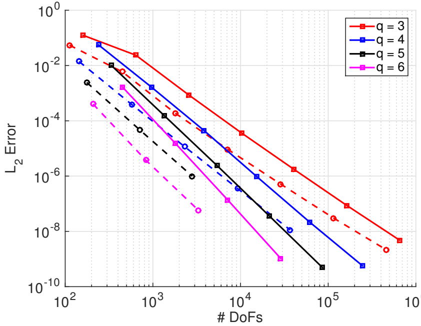

$\|u - u_{hp}\|_{L^2(\Omega)}$ vs. Degrees of Freedom (h-refinement)

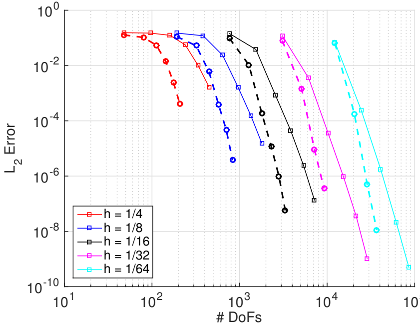

$\|u - u_{hp}\|_{L^2(\Omega)}$ vs. Degrees of Freedom (p-refinement)

Given a mesh $\mathcal{T}_h$ on Ω we derive the TDGFEM as follows.

TDGFEM for Helmholtz

Given a mesh $\mathcal{T}_h$ on Ω we derive the TDGFEM as follows.

- Multiply by test functions and integrate by parts, element-wise, twice (ultra weak formulation):

$$\int_K (-\Delta u - k^2 u)\, \bar{v} \quad d\boldsymbol{x} \qquad = 0$$

TDGFEM for Helmholtz

Given a mesh $\mathcal{T}_h$ on Ω we derive the TDGFEM as follows.

- Multiply by test functions and integrate by parts, element-wise, twice (ultra weak formulation):

$$\int_K (\nabla u \cdot \nabla \bar{v} - k^2 u \bar{v}) \, d\boldsymbol{x} \qquad - \int_{\partial K} \nabla u \cdot \boldsymbol{n}_K \bar{v} \, ds = 0$$

Given a mesh $\mathcal{T}_h$ on Ω we derive the TDGFEM as follows.

- Multiply by test functions and integrate by parts, element-wise, twice (ultra weak formulation):

$$\int_K u(-\Delta \bar{v} - k^2 \bar{v}) \; d\boldsymbol{x} + \int_{\partial K} u \nabla \bar{v} \cdot \boldsymbol{n}_K \, ds - \int_{\partial K} \nabla u \cdot \boldsymbol{n}_K \bar{v} \, ds = 0$$

TDGFEM for Helmholtz

Given a mesh $\mathcal{T}_h$ on Ω we derive the TDGFEM as follows.

- Multiply by test functions and integrate by parts, element-wise, twice (ultra weak formulation):

$$\int_K u(-\Delta \bar{v} - k^2 \bar{v}) \;\; d\boldsymbol{x} + \int_{\partial K} u \nabla \bar{v} \cdot \boldsymbol{n}_K \, ds - \int_{\partial K} \nabla u \cdot \boldsymbol{n}_K \bar{v} \, ds = 0$$

Given a mesh $\mathcal{T}_h$ on Ω we derive the TDGFEM as follows.

- Multiply by test functions and integrate by parts, element-wise, twice (ultra weak formulation):

$$\int_K u(-\Delta \bar{v} - k^2 \bar{v}) \; d\boldsymbol{x} + \int_{\partial K} u \nabla \bar{v} \cdot \boldsymbol{n}_K \, ds - \int_{\partial K} \nabla u \cdot \boldsymbol{n}_K \bar{v} \, ds = 0$$

- Replace continuous functions by discrete approximations ($u_{hp}, v_{hp} \in V_p(\mathcal{T}_h)$) and traces by numerical fluxes

$$u \to \widehat{u}_{hp}, \qquad \nabla u \to ik\widehat{\boldsymbol{\sigma}}_{hp}.$$

Given a mesh $\mathcal{T}_h$ on Ω we derive the TDGFEM as follows.

- Multiply by test functions and integrate by parts, element-wise, twice (ultra weak formulation):

$$\int_K u(-\Delta \bar{v} - k^2 \bar{v}) \ \ d\boldsymbol{x} + \int_{\partial K} u \nabla \bar{v} \cdot \boldsymbol{n}_K \, ds - \int_{\partial K} \nabla u \cdot \boldsymbol{n}_K \bar{v} \, ds = 0$$

- Replace continuous functions by discrete approximations ($u_{hp}, v_{hp} \in V_p(\mathcal{T}_h)$) and traces by numerical fluxes

$$u \to \widehat{u}_{hp}, \qquad \nabla u \to ik\widehat{\boldsymbol{\sigma}}_{hp}.$$

- $v \in V_p(\mathcal{T}_h) \subset T(\mathcal{T}_h) \quad \Longrightarrow \quad -\Delta \bar{v} - k^2 \bar{v} = 0$ in K.

Given a mesh $\mathcal{T}_h$ on Ω we derive the TDGFEM as follows.

- Multiply by test functions and integrate by parts, element-wise, twice (ultra weak formulation):

$$\int_K u(-\Delta \bar{v} - k^2 \bar{v}) \; d\boldsymbol{x} + \int_{\partial K} u \nabla \bar{v} \cdot \boldsymbol{n}_K \, ds - \int_{\partial K} \nabla u \cdot \boldsymbol{n}_K \bar{v} \, ds = 0$$

- Replace continuous functions by discrete approximations $(u_{hp}, v_{hp} \in V_p(\mathcal{T}_h))$ and traces by numerical fluxes

$$u \to \widehat{u}_{hp}, \qquad \nabla u \to ik\widehat{\boldsymbol{\sigma}}_{hp}.$$

- $v \in V_p(\mathcal{T}_h) \subset T(\mathcal{T}_h) \quad \Longrightarrow \quad -\Delta \bar{v} - k^2 \bar{v} = 0$ in K.

$$\int_{\partial K} \widehat{u}_{hp} \nabla \bar{v}_{hp} \cdot \boldsymbol{n}_K \, ds - \int_{\partial K} ik\widehat{\boldsymbol{\sigma}}_{hp} \cdot \boldsymbol{n}_K \bar{v}_{hp} \, ds = 0, \qquad \text{for all } K \in \mathcal{T}_h.$$

Trefftz Discontinuous Galerkin FEM for Helmholtz

Find $u_{hp} \in V_p(\mathcal{T}_h)$ such that,

$$\mathcal{A}_h(u_{hp}, v_{hp}) = \ell_h(v_{hp}),$$

for all $v_{hp} \in V_p(\mathcal{T}_h)$, where

$$\begin{aligned}
\mathcal{A}_h(u,v) = &\int_{\mathcal{F}_h^I \cup \mathcal{F}_h^N} \{\!\{u\}\!\} [\![\nabla_h \bar{v}]\!] \, ds - \int_{\mathcal{F}_h^I \cup \mathcal{F}_h^N} \beta (ik)^{-1} [\![\nabla_h u]\!] [\![\nabla_h \bar{v}]\!] \, ds \\
&- \int_{\mathcal{F}_h^I \cup \mathcal{F}_h^D} \{\!\{\nabla_h u\}\!\} \cdot [\![\bar{v}]\!] \, ds + \int_{\mathcal{F}_h^I \cup \mathcal{F}_h^D} \alpha ik [\![u]\!] \cdot [\![\bar{v}]\!] \, ds \\
&+ \int_{\mathcal{F}_h^R} (1-\delta) u \nabla_h \bar{v} \cdot \boldsymbol{n} \, ds - \int_{\mathcal{F}_h^R} \delta (ik\vartheta)^{-1} (\nabla_h u \cdot \boldsymbol{n})(\nabla_h \bar{v} \cdot \boldsymbol{n}) \, ds \\
&- \int_{\mathcal{F}_h^R} \delta \nabla_h u \cdot \boldsymbol{n} \bar{v} \, ds + \int_{\mathcal{F}_h^R} (1-\delta) ik\vartheta u \bar{v} \, ds, \\
\ell_h(v) = &- \int_{\mathcal{F}_h^R} \delta (ik\vartheta)^{-1} g_R \nabla_h \bar{v} \cdot \boldsymbol{n} \, ds + \int_{\mathcal{F}_h^R} (1-\delta) g_R \bar{v} \, ds.
\end{aligned}$$

Flux Parameters

Penalty Type	α	β	δ
DG-type Gittelson, Hiptmair & Perugia, 2009	$\mathtt{a}q_K^2/kh_K$	$\mathtt{b}kh_K/q_K$	$\mathtt{d}kh_K/q_K$
Constant Hiptmair, Moiola & Perugia, 2011	$\mathtt{a}$	$\mathtt{b}$	$\mathtt{d}$
UWVF Cessenat & Després, 1998	$1/2$	$1/2$	$1/2$
Non-Uniform Mesh Hiptmair, Moiola & Perugia, 2014	$\mathtt{a}h_{\max}/h_K$	$\mathtt{b}h_{\max}/h_K$	$\mathtt{d}h_{\max}/h_K$

For the rest of this talk we ignore Neumann boundary conditions.

Flux Parameters

Penalty Type	α	β	δ
DG-type Gittelson, Hiptmair & Perugia, 2009	$\mathtt{a}q_K^2/kh_K$	$\mathtt{b}kh_K/q_K$	$\mathtt{d}kh_K/q_K$
Constant Hiptmair, Moiola & Perugia, 2011	$\mathtt{a}$	$\mathtt{b}$	$\mathtt{d}$
UWVF Cessenat & Després, 1998	$1/2$	$1/2$	$1/2$
Non-Uniform Mesh Hiptmair, Moiola & Perugia, 2014	$\mathtt{a}h_{\max}/h_K$	$\mathtt{b}h_{\max}/h_K$	$\mathtt{d}h_{\max}/h_K$

For the rest of this talk we ignore Neumann boundary conditions.

Energy Norm

$$\left\| v \right\|_{\mathrm{TDG}}^2 = k\left\| \alpha^{1/2} [\![v]\!] \right\|_{L^2(\mathcal{F}_h^I \cup \mathcal{F}_h^D)}^2 + \frac{1}{k}\left\| \beta^{\frac{1}{2}} [\![\nabla v]\!] \right\|_{L^2(\mathcal{F}_h^I)}^2 + \frac{1}{k\vartheta}\left\| \delta^{1/2} \nabla v \cdot \boldsymbol{n}_K \right\|_{L^2(\mathcal{F}_h^R)}^2 + k\vartheta \left\| (1-\delta)^{1/2} v \right\|_{L^2(\mathcal{F}_h^R)}^2$$

Define the weighted Sobolev norm

$$\|v\|_{H^s(\Omega),k} = \sum_{j=0}^{s} k^{2(s-j)} |v|^2_{H^j(\Omega)}.$$

Theorem (*a priori* — Non-Uniform Mesh & Non-Uniform Parameters)

Let u be the analytical solution with $u|_K \in H^{s_K+1}(K)$, u_{hp} the TDG solution. For sufficiently large q_K (and assuming $q_K > 2s_K + 1$)

$$\|u - u_p\|_{L^2(\Omega)} \le C d_\Omega^2 [(d_\Omega k)^{-1} + (d_\Omega^{-1} h)^{s_K + 1/2}] \times \sum_{K \in \mathcal{T}_h} C_K h_K^{s_K - 1} \left(\frac{1}{\widehat{q}_K}\right)^{s_K - 1/2} \|u\|_{H^{s+1}(\Omega),k},$$

where C_K depends on kh_K (as an increasing function) and s_K. Here, $\widehat{q}_K = q_K / \log(q_k + 2)$. [Hiptmair, Moiola & Perugia, 2014]

Consider the smooth (analytic) solution (for Acoustic Wave Propagation)

$$u(r,\theta) = \mathcal{J}_1(kr)\cos(\theta)$$

on the domain $\Omega = (0,1) \times (-1/2, 1/2)$.

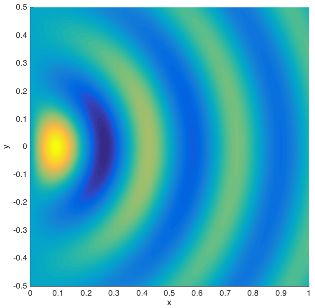

Re(Anal. Soln.) (k=20)

Comparison of Flux Parameters (2D)

Consider the smooth (analytic) solution (for Acoustic Wave Propagation)

$$u(r,\theta) = \mathcal{J}_1(kr)\cos(\theta)$$

on the domain $\Omega = (0,1) \times (-1/2, 1/2)$.
We solve using constant (solid line) and DG-type parameters (dashed).

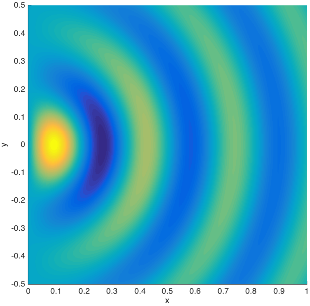

Re(Anal. Soln.) (k=20)

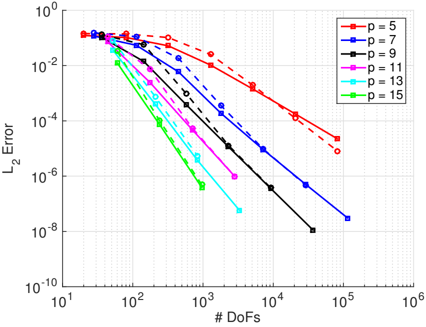

$k = 20$

To test the non-uniform parameters, we consider the solution

$$u(x,y) = \mathcal{H}_0^{(1)}(k\sqrt{x^2+y^2}),$$

with $k = 50$, on the domain $\Omega = (0,1)^2$, where $\mathcal{H}_0^{(1)}$ represents the Hankel function of the first kind of order 0.

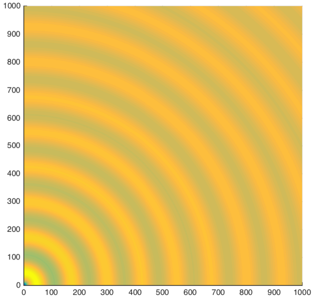

Im(Anal. Soln.)

To test the non-uniform parameters, we consider the solution

$$u(x, y) = \mathcal{H}_0^{(1)}(k\sqrt{x^2 + y^2}),$$

with $k = 50$, on the domain $\Omega = (0, 1)^2$, where $\mathcal{H}_0^{(1)}$ represents the Hankel function of the first kind of order 0.

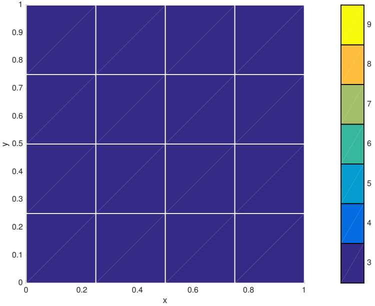

Mesh 1

To test the non-uniform parameters, we consider the solution

$$u(x, y) = \mathcal{H}_0^{(1)}(k\sqrt{x^2 + y^2}),$$

with $k = 50$, on the domain $\Omega = (0, 1)^2$, where $\mathcal{H}_0^{(1)}$ represents the Hankel function of the first kind of order 0.

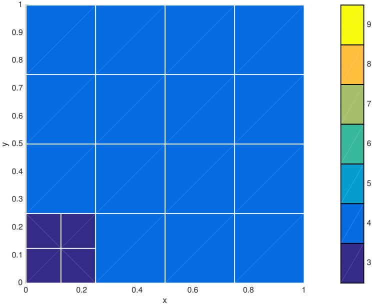

Mesh 2

To test the non-uniform parameters, we consider the solution

$$u(x, y) = \mathcal{H}_0^{(1)}(k\sqrt{x^2 + y^2}),$$

with $k = 50$, on the domain $\Omega = (0, 1)^2$, where $\mathcal{H}_0^{(1)}$ represents the Hankel function of the first kind of order 0.

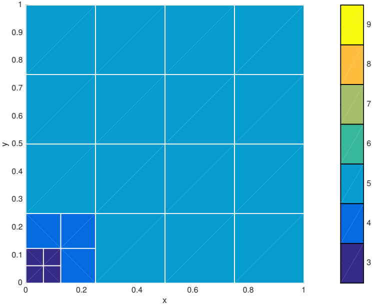

Mesh 3

Comparison of Flux Parameters (Non-Unif.)

To test the non-uniform parameters, we consider the solution

$$u(x,y) = \mathcal{H}_0^{(1)}(k\sqrt{x^2+y^2}),$$

with $k = 50$, on the domain $\Omega = (0,1)^2$, where $\mathcal{H}_0^{(1)}$ represents the Hankel function of the first kind of order 0.

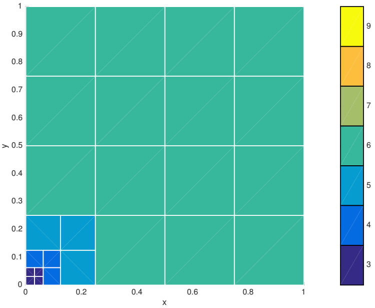

Mesh 4

To test the non-uniform parameters, we consider the solution

$$u(x,y) = \mathcal{H}_0^{(1)}(k\sqrt{x^2+y^2}),$$

with $k = 50$, on the domain $\Omega = (0,1)^2$, where $\mathcal{H}_0^{(1)}$ represents the Hankel function of the first kind of order 0.

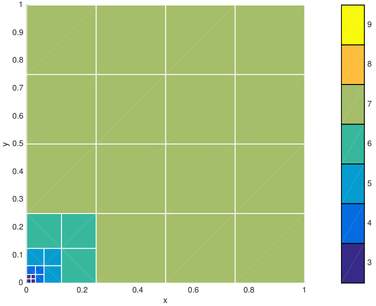

Mesh 5

Comparison of Flux Parameters (Non-Unif.)

To test the non-uniform parameters, we consider the solution

$$u(x, y) = \mathcal{H}_0^{(1)}(k\sqrt{x^2 + y^2}),$$

with $k = 50$, on the domain $\Omega = (0, 1)^2$, where $\mathcal{H}_0^{(1)}$ represents the Hankel function of the first kind of order 0.

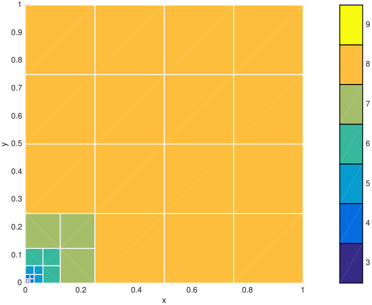

Mesh 6

To test the non-uniform parameters, we consider the solution

$$u(x, y) = \mathcal{H}_0^{(1)}(k\sqrt{x^2 + y^2}),$$

with $k = 50$, on the domain $\Omega = (0, 1)^2$, where $\mathcal{H}_0^{(1)}$ represents the Hankel function of the first kind of order 0.

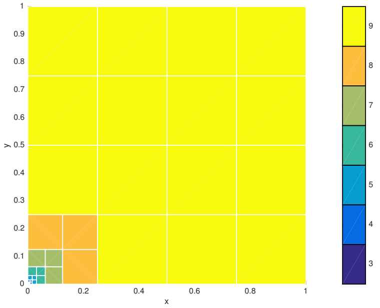

Mesh 7

To test the non-uniform parameters, we consider the solution

$$u(x,y) = \mathcal{H}_0^{(1)}(k\sqrt{x^2+y^2}),$$

with $k = 50$, on the domain $\Omega = (0,1)^2$, where $\mathcal{H}_0^{(1)}$ represents the Hankel function of the first kind of order 0.

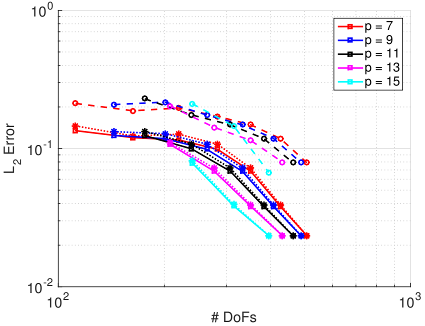

Constant (solid line), DG-type (dashed) & non-uniform (dotted) parameters

Plane Wave Direction Refinement

Consider a plane wave analytical solution (for Acoustic Wave Propagation)

$$u(\boldsymbol{x}) = \mathrm{e}^{ik\boldsymbol{d}\cdot\boldsymbol{x}}$$

for $k = 20$ on the domain $\Omega = (0,1)^2$, where $\boldsymbol{d} = (1/\sqrt{2}, 1/\sqrt{2})$.

Consider a plane wave analytical solution (for Acoustic Wave Propagation)

$$u(\boldsymbol{x}) = \mathrm{e}^{ik\boldsymbol{d}\cdot\boldsymbol{x}}$$

for $k = 20$ on the domain $\Omega = (0,1)^2$, where $\boldsymbol{d} = (1/\sqrt{2}, 1/\sqrt{2})$.
We evenly distribute directions $\boldsymbol{d}_\ell$, starting from $\boldsymbol{d}_1 = (1,0)$.

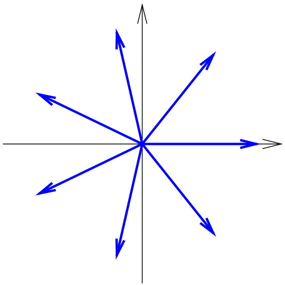

Plane Wave Directions ($q = 3$)

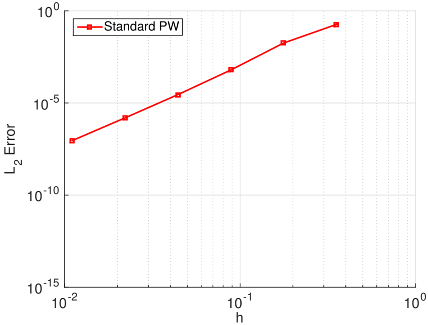

$\|u - u_{hp}\|_{L^2(\Omega)}$ vs. h

Consider a plane wave analytical solution (for Acoustic Wave Propagation)

$$u(\boldsymbol{x}) = \mathrm{e}^{ik\boldsymbol{d}\cdot\boldsymbol{x}}$$

for $k = 20$ on the domain $\Omega = (0,1)^2$, where $\boldsymbol{d} = (1/\sqrt{2}, 1/\sqrt{2})$.
We evenly distribute directions $\boldsymbol{d}_\ell$, starting from $\boldsymbol{d}_1 = (1,0)$.
Rotating directions so that $\boldsymbol{d}_1 = \boldsymbol{d}$ (almost) gives the analytical solution.

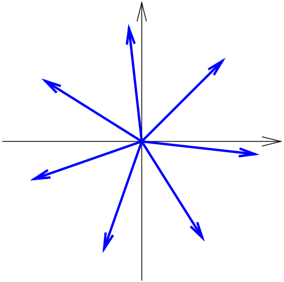

Rotated Directions ($q = 3$)

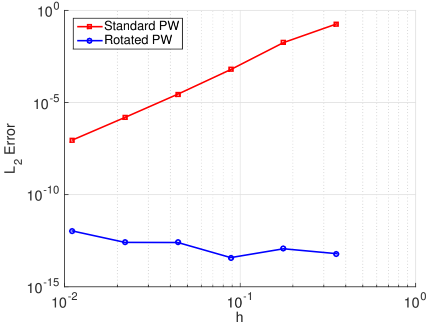

$\left\|u - u_{hp}\right\|_{L^2(\Omega)}$ vs. h

Plane Wave Direction Refinement

Even for non-plane wave solutions the analytical solutions picking the correct main direction reduces the error.

Plane Wave Direction Refinement

Even for non-plane wave solutions the analytical solutions picking the correct main direction reduces the error.

We need a way calculate/adapt the directions without the analytical solution. Several existing approaches exist:

- Ray-tracing — requires a source term. [Betcke & Phillips, 2012]
- Approximate
$$\frac{\nabla e(\boldsymbol{x}_0)}{ike(\boldsymbol{x}_0)},$$
where e is the error. [Gittelson, 2008 (Master's Thesis)]
- Adding an extra unknown (the optimal angle of rotation) to the basis functions. [Amara, Chaudhry, Diaz, Djellouli & Fiedler, 2014]

Plane Wave Direction Refinement

Even for non-plane wave solutions the analytical solutions picking the correct main direction reduces the error.

We need a way calculate/adapt the directions without the analytical solution. Several existing approaches exist:

- Ray-tracing — requires a source term. [Betcke & Phillips, 2012]
- Approximate
$$\frac{\nabla e(\boldsymbol{x}_0)}{ike(\boldsymbol{x}_0)},$$
where e is the error. [Gittelson, 2008 (Master's Thesis)]
- Adding an extra unknown (the optimal angle of rotation) to the basis functions. [Amara, Chaudhry, Diaz, Djellouli & Fiedler, 2014]

We propose using the Hessian of the numerical solution, based on work on anisotropic meshes for standard FE [Formaggia & Perotto, 2001, 2003].

Plane Wave Direction Refinement

Even for non-plane wave solutions the analytical solutions picking the correct main direction reduces the error.

We need a way calculate/adapt the directions without the analytical solution. Several existing approaches exist:

- Ray-tracing — requires a source term. [Betcke & Phillips, 2012]
- Approximate

$$\frac{\nabla e(\boldsymbol{x}_0)}{ike(\boldsymbol{x}_0)},$$

  where e is the error. [Gittelson, 2008 (Master's Thesis)]
- Adding an extra unknown (the optimal angle of rotation) to the basis functions. [Amara, Chaudhry, Diaz, Djellouli & Fiedler, 2014]

We propose using the Hessian of the numerical solution, based on work on anisotropic meshes for standard FE [Formaggia & Perotto, 2001, 2003].

The eigenvector of the Hessian matching the largest eigenvalue should be the direction to use as the main direction, assuming the matching eigenvalue is significantly larger.

Plane Wave Refinement Algorithm (2D)

Let $(\lambda_1, \boldsymbol{v}_1), (\lambda_2, \boldsymbol{v}_2)$ be the eigenpairs of $\mathbf{H}(\mathrm{Re}(u_h(\boldsymbol{x}_K)))$, and $(\mu_1, \boldsymbol{w}_1), (\mu_2, \boldsymbol{w}_2)$ the eigenpairs of $\mathbf{H}(\mathrm{Im}(u_h(\boldsymbol{x}_K)))$ s.t. $\lambda_1 \geq \lambda_2$, $\mu_1 \geq \mu_2$; then, for constant $C > 1$, we can select the first plane wave direction as follows:

$\lambda_1 \geq C\lambda_2$	$\mu_1 \geq C\mu_2$	$\lambda_1 \geq C\mu_1$	$\mu_1 \geq C\lambda_1$	First PW Direction
✓	✓	✓	✗	$\boldsymbol{v}_1$
✓	✓	✗	✓	$\boldsymbol{w}_1$
✓	✓	✗	✗	$(\boldsymbol{v}_1+\boldsymbol{w}_1)/2$
✓	✗	✓	✗	$\boldsymbol{v}_1$
✓	✗	✗	–	–
✗	✓	✗	✓	$\boldsymbol{w}_1$
✗	✓	–	✗	–
✗	✗	–	–	–

If $\boldsymbol{v}$ is the eigenvector, then the direction of propagation could be either $\boldsymbol{v}$ or $-\boldsymbol{v}$ (unknown orientation). Consider the impedance on the boundary of a ball (radius δ around $\boldsymbol{x}_K$) and compare to the plane wave $u(\boldsymbol{x}) = \mathrm{e}^{ik\boldsymbol{d}\cdot(\boldsymbol{x}-\boldsymbol{x}_K)}$ for the cases when $\boldsymbol{d} = \boldsymbol{v}$ and $\boldsymbol{d} = -\boldsymbol{v}$.

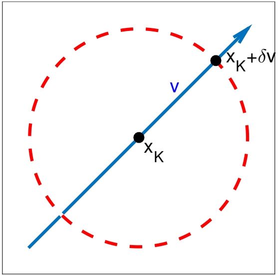

Plane Wave Direction Refinement

If $\boldsymbol{v}$ is the eigenvector, then the direction of propagation could be either $\boldsymbol{v}$ or $-\boldsymbol{v}$ (unknown orientation). Consider the impedance on the boundary of a ball (radius δ around $\boldsymbol{x}_K$) and compare to the plane wave $u(\boldsymbol{x}) = \mathrm{e}^{ik\boldsymbol{d}\cdot(\boldsymbol{x}-\boldsymbol{x}_K)}$ for the cases when $\boldsymbol{d} = \boldsymbol{v}$ and $\boldsymbol{d} = -\boldsymbol{v}$.

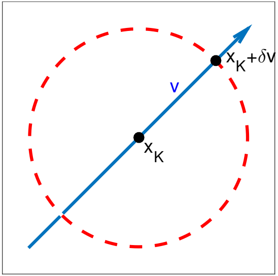

Evaluating at $\boldsymbol{x}_K + \delta\boldsymbol{v}$ we note that the normal is $\boldsymbol{v}$, so we can calculate

$$\frac{\nabla u_h(\boldsymbol{x}_K)\cdot\boldsymbol{v} + iku_h(\boldsymbol{x}_K)}{iku_h(\boldsymbol{x}_K)}.$$

If $\boldsymbol{v}$ is the eigenvector, then the direction of propagation could be either $\boldsymbol{v}$ or $-\boldsymbol{v}$ (unknown orientation). Consider the impedance on the boundary of a ball (radius δ around $\boldsymbol{x}_K$) and compare to the plane wave $u(\boldsymbol{x}) = \mathrm{e}^{ik\boldsymbol{d}\cdot(\boldsymbol{x}-\boldsymbol{x}_K)}$ for the cases when $\boldsymbol{d} = \boldsymbol{v}$ and $\boldsymbol{d} = -\boldsymbol{v}$.

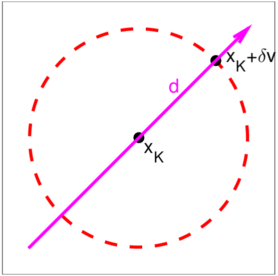

Evaluating at $\boldsymbol{x}_K + \delta\boldsymbol{v}$ we note that the normal is $\boldsymbol{v}$, so we can calculate

$$\frac{\nabla u_h(\boldsymbol{x}_K)\cdot\boldsymbol{v} + iku_h(\boldsymbol{x}_K)}{iku_h(\boldsymbol{x}_K)}.$$

We can compare this to the impedance for the u:

$$\frac{\nabla u(\boldsymbol{x}_K)\cdot\boldsymbol{v} + iku(\boldsymbol{x}_K)}{iku(\boldsymbol{x}_K)} = \begin{cases} 2, & \text{if } \boldsymbol{d} = \boldsymbol{v}, \\ & \end{cases}$$

If $\boldsymbol{v}$ is the eigenvector, then the direction of propagation could be either $\boldsymbol{v}$ or $-\boldsymbol{v}$ (unknown orientation). Consider the impedance on the boundary of a ball (radius δ around $\boldsymbol{x}_K$) and compare to the plane wave $u(\boldsymbol{x}) = \mathrm{e}^{ik\boldsymbol{d}\cdot(\boldsymbol{x}-\boldsymbol{x}_K)}$ for the cases when $\boldsymbol{d} = \boldsymbol{v}$ and $\boldsymbol{d} = -\boldsymbol{v}$.

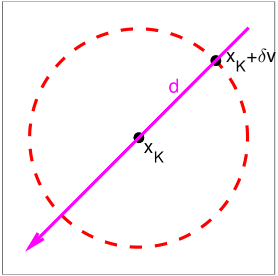

Evaluating at $\boldsymbol{x}_K + \delta\boldsymbol{v}$ we note that the normal is $\boldsymbol{v}$, so we can calculate

$$\frac{\nabla u_h(\boldsymbol{x}_K)\cdot\boldsymbol{v} + iku_h(\boldsymbol{x}_K)}{iku_h(\boldsymbol{x}_K)}.$$

We can compare this to the impedance for the u:

$$\frac{\nabla u(\boldsymbol{x}_K)\cdot\boldsymbol{v} + iku(\boldsymbol{x}_K)}{iku(\boldsymbol{x}_K)} = \begin{cases} 2, & \text{if } \boldsymbol{d} = \boldsymbol{v}, \\ 0, & \text{if } \boldsymbol{d} = -\boldsymbol{v}. \end{cases}$$

To test the direction refinement, we consider the solution

$$u(x,y) = \mathcal{H}_0^{(1)}(k\sqrt{(x+0.25)^2+y^2}),$$

with $k = 20$, on the domain $\Omega = (0,1)^2$.

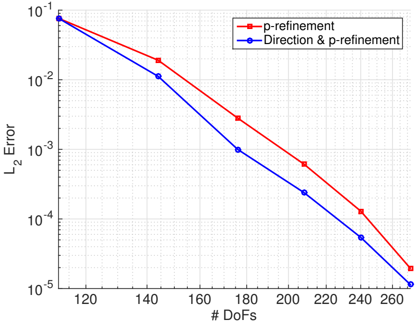

$\|u - u_{hp}\|_{L^2(\Omega)}$ vs. DoF

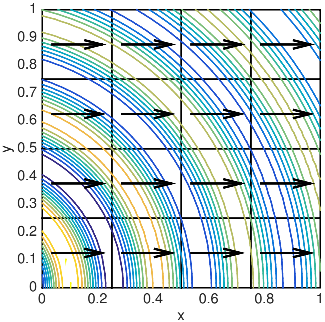

First PW Direction ($p = 3$)

Plane Wave Direction Refinement

To test the direction refinement, we consider the solution

$$u(x,y) = \mathcal{H}_0^{(1)}(k\sqrt{(x+0.25)^2+y^2}),$$

with $k = 20$, on the domain $\Omega = (0,1)^2$.

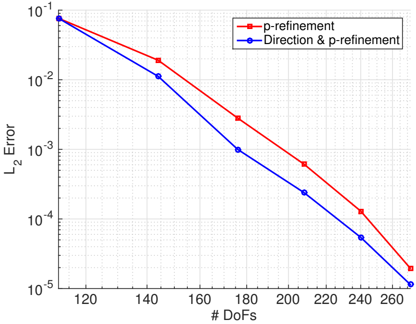

$\|u - u_{hp}\|_{L^2(\Omega)}$ vs. *DoF*

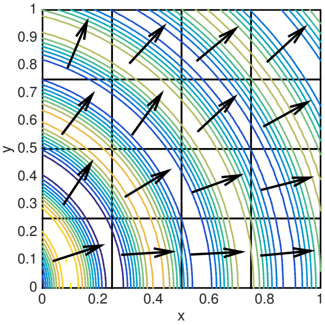

First PW Direction ($p = 4$)

To test the direction refinement, we consider the solution

$$u(x,y) = \mathcal{H}_0^{(1)}(k\sqrt{(x+0.25)^2+y^2}),$$

with $k = 20$, on the domain $\Omega = (0,1)^2$.

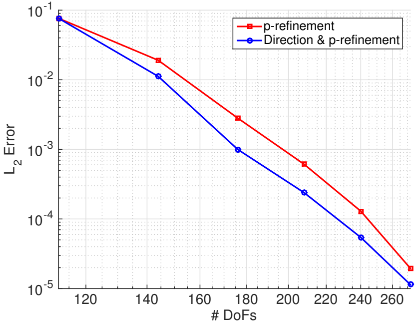

$\|u - u_{hp}\|_{L^2(\Omega)}$ vs. *DoF*

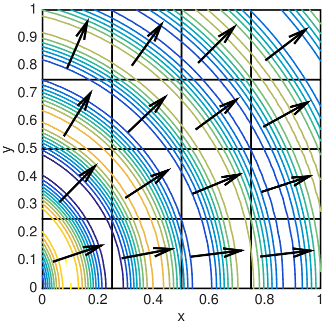

First PW Direction ($p = 5$)

universität wien

To test the direction refinement, we consider the solution

$$u(x,y) = \mathcal{H}_0^{(1)}(k\sqrt{(x+0.25)^2+y^2}),$$

with $k = 20$, on the domain $\Omega = (0,1)^2$.

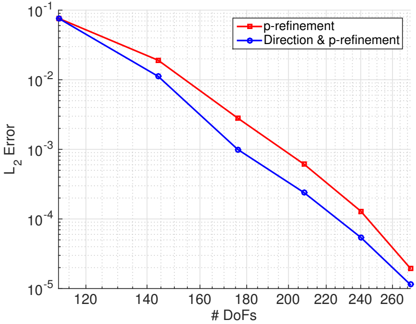

$\|u - u_{hp}\|_{L^2(\Omega)}$ vs. DoF

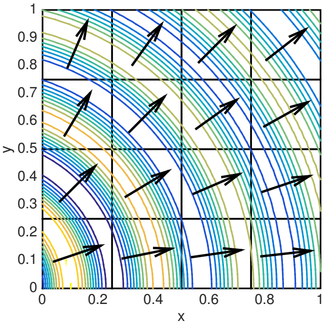

First PW Direction ($p = 6$)

Plane Wave Direction Refinement

To test the direction refinement, we consider the solution

$$u(x,y) = \mathcal{H}_0^{(1)}(k\sqrt{(x+0.25)^2+y^2}),$$

with $k = 20$, on the domain $\Omega = (0,1)^2$.

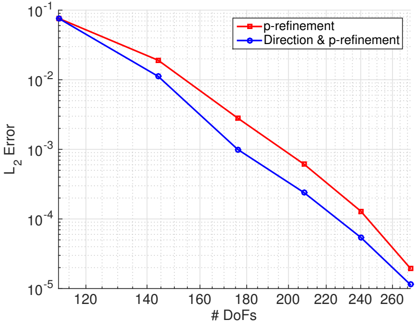

$\|u - u_{hp}\|_{L^2(\Omega)}$ vs. *DoF*

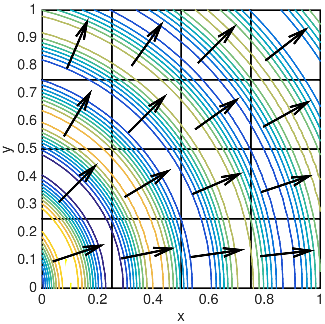

First PW Direction ($p = 7$)

Plane Wave Direction Refinement

To test the direction refinement, we consider the solution

$$u(x,y) = \mathcal{H}_0^{(1)}(k\sqrt{(x+0.25)^2 + y^2}),$$

with $k = 20$, on the domain $\Omega = (0,1)^2$.

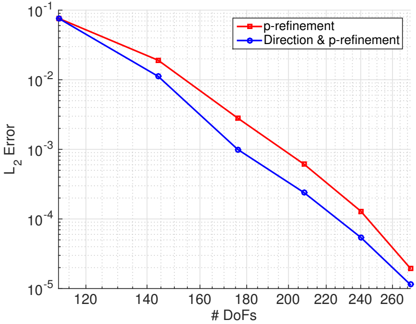

$\|u - u_{hp}\|_{L^2(\Omega)}$ vs. *DoF*

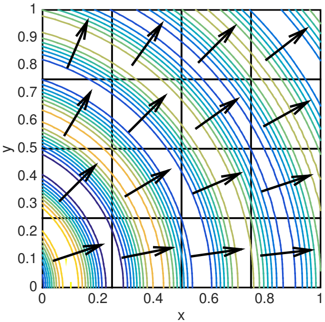

First PW Direction ($p = 8$)

A posteriori Error Estimates

Ignoring Neumann boundary conditions *a posteriori* error bounds exists for the *h*-version of the method in $\mathbb{R}^2$.

Ignoring Neumann boundary conditions *a posteriori* error bounds exists for the h-version of the method in $\mathbb{R}^2$.

A posteriori Error Bound — h-version Only

For the TDGFEM, with the non-uniform flux parameters, the following error bound holds:

$$\|u - u_{hp}\|_{L^2(\Omega)} \leq C \left\{ \left\| \alpha^{1/2} h_F^s [\![u_h]\!] \right\|_{L^2(\mathcal{F}_h^I \cup \mathcal{F}_h^D)} + \frac{1}{k} \| \beta^{\frac{1}{2}} h_F^s [\![\nabla u_h]\!] \|_{L^2(\mathcal{F}_h^I)} + \frac{1}{k} \left\| \delta^{1/2} h_F^s \left(g_R - \nabla u_h \cdot \boldsymbol{n}_K + ik\vartheta u_h \right) \right\|_{L^2(\mathcal{F}_h^R)} \right\}$$

where s depends on the regularity of the solution to the adjoint problem ($z \in H^{3/2+s}(\Omega)$).

[Kapita, Monk, Warburton (2014 - Tech. Report)]

Consider again the solution

$$u(x,y) = H_0^{(1)}(k(x^2+y^2)),$$

with $k = 50$, on the domain $\Omega = (0,1)^2$.
We solve using constant (solid line), DG-type (dashed) and non-uniform parameter (dotted).

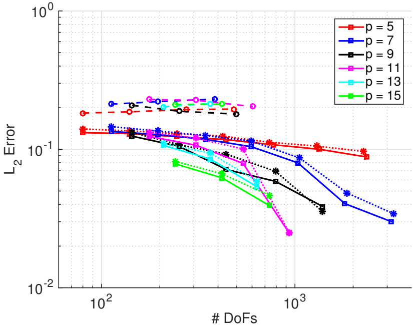

L_2 Error

Consider again the solution

$$u(x,y) = H_0^{(1)}(k(x^2+y^2)),$$

with $k = 50$, on the domain $\Omega = (0,1)^2$.
We solve using constant (solid line), DG-type (dashed) and non-uniform parameter (dotted).

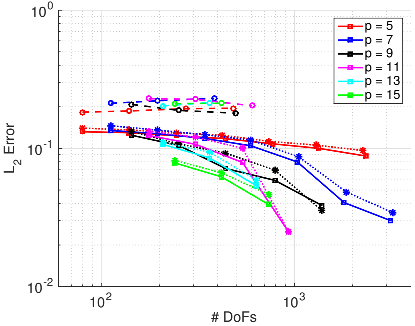

L_2 Error

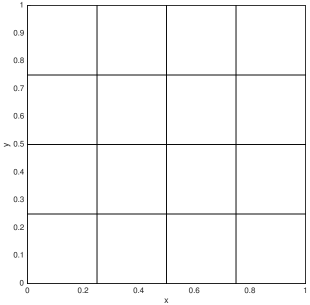

Mesh ($p = 3$)

Consider again the solution

$$u(x, y) = H_0^{(1)}(k(x^2 + y^2)),$$

with $k = 50$, on the domain $\Omega = (0, 1)^2$.
We solve using constant (solid line), DG-type (dashed) and non-uniform parameter (dotted).

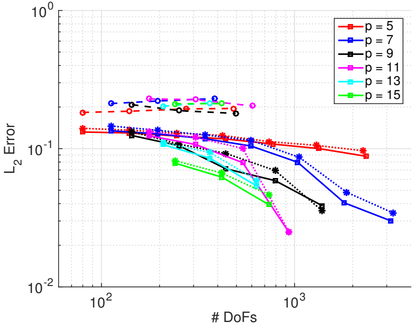

L_2 Error

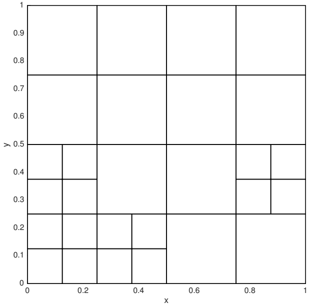

Mesh $(p = 4)$

Adaptive Refinement

Consider again the solution

$$u(x,y) = H_0^{(1)}(k(x^2+y^2)),$$

with $k = 50$, on the domain $\Omega = (0,1)^2$.
We solve using constant (solid line), DG-type (dashed) and non-uniform parameter (dotted).

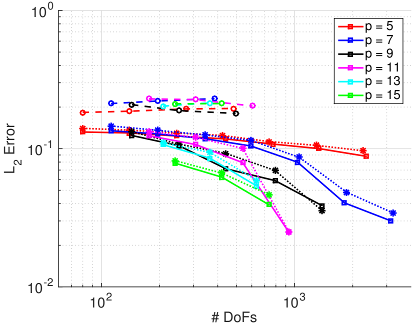

L_2 Error

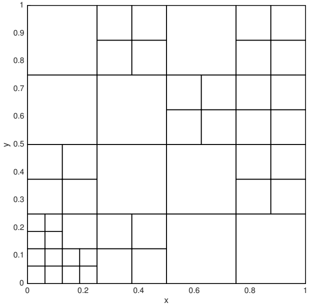

Mesh ($p = 5$)

Consider again the solution

$$u(x, y) = H_0^{(1)}(k(x^2 + y^2)),$$

with $k = 50$, on the domain $\Omega = (0, 1)^2$.
We solve using constant (solid line), DG-type (dashed) and non-uniform parameter (dotted).

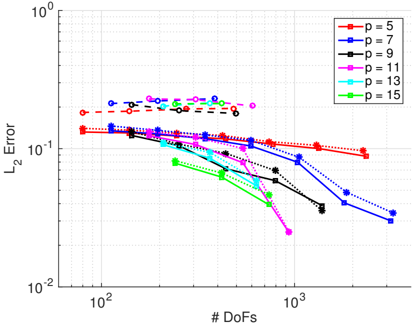

L_2 Error

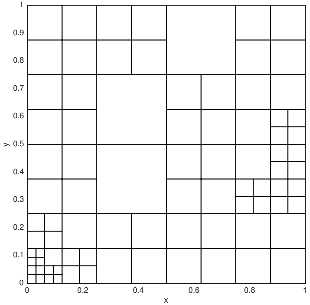

Mesh ($p = 6$)

Consider again the solution

$$u(x,y) = H_0^{(1)}(k(x^2 + y^2)),$$

with $k = 50$, on the domain $\Omega = (0,1)^2$.
We solve using constant (solid line), DG-type (dashed) and non-uniform parameter (dotted).

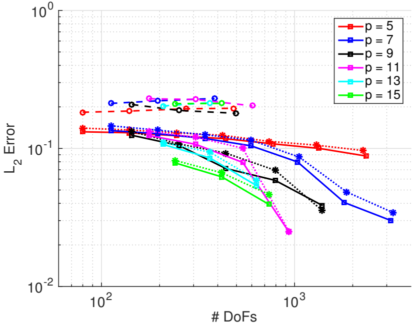

L_2 Error

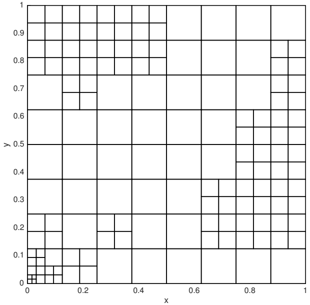

Mesh ($p = 7$)

Consider again the solution

$$u(x,y) = H_0^{(1)}(k(x^2 + y^2)),$$

with $k = 50$, on the domain $\Omega = (0,1)^2$.
We solve using constant (solid line), DG-type (dashed) and non-uniform parameter (dotted).

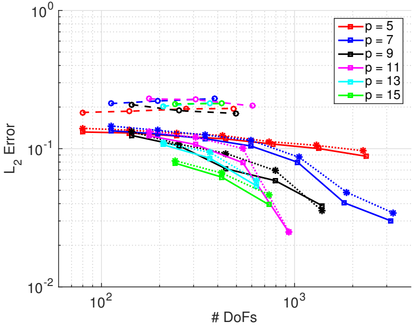

L_2 Error

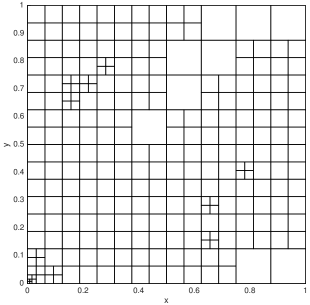

Mesh ($p = 8$)

Summary:

- *A priori* results exist for Trefftz DG, with Robin and Dirichlet BCs

Conclusion

Summary:

- *A priori* results exist for Trefftz DG, with Robin and Dirichlet BCs
- Various choice of flux parameters is required for the existing analysis

Summary:

- *A priori* results exist for Trefftz DG, with Robin and Dirichlet BCs
- Various choice of flux parameters is required for the existing analysis
- The choice of flux parameters tends to make no difference on smooth solutions, although DG-style parameters appear poor for non-uniform refinement/singular problems.

Conclusion

Summary:

- *A priori* results exist for Trefftz DG, with Robin and Dirichlet BCs
- Various choice of flux parameters is required for the existing analysis
- The choice of flux parameters tends to make no difference on smooth solutions, although DG-style parameters appear poor for non-uniform refinement/singular problems.
- With plane wave basis functions it is possible to refine the wave directions.

Conclusion

Summary:

- *A priori* results exist for Trefftz DG, with Robin and Dirichlet BCs
- Various choice of flux parameters is required for the existing analysis
- The choice of flux parameters tends to make no difference on smooth solutions, although DG-style parameters appear poor for non-uniform refinement/singular problems.
- With plane wave basis functions it is possible to refine the wave directions.

Future Aims:

Conclusion

Summary:

- *A priori* results exist for Trefftz DG, with Robin and Dirichlet BCs
- Various choice of flux parameters is required for the existing analysis
- The choice of flux parameters tends to make no difference on smooth solutions, although DG-style parameters appear poor for non-uniform refinement/singular problems.
- With plane wave basis functions it is possible to refine the wave directions.

Future Aims:

- Extend the existing *a posteriori* error analysis to *hp*-version meshes (ideally for constant flux parameters).

Conclusion

Summary:

- *A priori* results exist for Trefftz DG, with Robin and Dirichlet BCs
- Various choice of flux parameters is required for the existing analysis
- The choice of flux parameters tends to make no difference on smooth solutions, although DG-style parameters appear poor for non-uniform refinement/singular problems.
- With plane wave basis functions it is possible to refine the wave directions.

Future Aims:

- Extend the existing *a posteriori* error analysis to *hp*-version meshes (ideally for constant flux parameters).
- Develop an algorithm for deciding on whether to perform h or p refinement.

Conclusion

Summary:

- *A priori* results exist for Trefftz DG, with Robin and Dirichlet BCs
- Various choice of flux parameters is required for the existing analysis
- The choice of flux parameters tends to make no difference on smooth solutions, although DG-style parameters appear poor for non-uniform refinement/singular problems.
- With plane wave basis functions it is possible to refine the wave directions.

Future Aims:

- Extend the existing *a posteriori* error analysis to *hp*-version meshes (ideally for constant flux parameters).
- Develop an algorithm for deciding on whether to perform h or p refinement.
- Use the eigenvalues/eigenvectors to develop *anisotropic* p-refinement (unevenly spaced plane waves).